

Electron scattering by the hydrocarbons C_4H_6 , C_5H_8 , and C_6H_{10}

Matheus B. Kiataki, Diego F. Pastega, and Márcio H. F. Bettega

Departamento de Física, Universidade Federal do Paraná, Caixa Postal 19044, 81531-990 Curitiba, Paraná, Brazil

(Received 23 August 2017; published 17 October 2017)

We report calculated elastic integral and differential cross sections for electron collisions with the hydrocarbons 1,3-butadiene (C_4H_6), 2-methyl-1,3-butadiene (C_5H_8), and 2,3-dimethyl-1,3-butadiene (C_6H_{10}) for impact energies up to 15 eV. Our calculations were performed with the Schwinger Multichannel Method with pseudopotentials, in the static-exchange and static-exchange plus polarization approximations. These molecules differ for the presence of one methyl group, in the case of C_5H_8 , and two methyl groups, in the case of C_6H_{10} in substitution of one and two hydrogen atoms in C_4H_6 , respectively (methylation effect). For the polar molecule 2-methyl-1,3-butadiene, we included the Born closure procedure in order to account for the long-range potential. We found two π^* shape resonances in the integral cross section of each one of the molecules studied. The present results are also compared with the experimental values for the resonances positions and with total cross sections available in the literature. In particular, we show that the minimum in the total cross section of C_5H_8 located at around 1.6 eV and assigned by the authors as a Ramsauer-Townsend minimum is, actually, a valley between the two π^* shape resonances. Also for the C_5H_8 molecule, the enhancement in the total cross section below 1.6 eV is the tail of the low-lying shape resonance and not an effect due to its permanent dipole moment, as suggested by the authors. We discuss the influence of the methylation effect in the shape and magnitude of the elastic cross sections and also in the location of the π^* shape resonances of these hydrocarbons.

DOI: [10.1103/PhysRevA.96.042711](https://doi.org/10.1103/PhysRevA.96.042711)

I. INTRODUCTION

Electron interactions with hydrocarbons has been the subject of several theoretical and experimental studies [1]. These investigations considered all types of collisions (total, elastic, inelastic, ionization). The presence of shape resonances, Ramsauer-Townsend minimum, and virtual state in the integral and total cross sections has been discussed. Another topic that has been investigated is the relation between the oscillatory behavior of the differential cross sections and the type molecular chain (straight versus branched) [2].

The focus of the present work is on elastic scattering of low-energy electrons with the hydrocarbons 1,3-butadiene (C_4H_6), 2-methyl-1,3-butadiene (C_5H_8), and 2,3-dimethyl-1,3-butadiene (C_6H_{10}). These hydrocarbons differ from each other by the presence of one and two methyl groups, in the case of C_5H_8 , and C_6H_{10} , in substitution of one and two hydrogen atoms in C_4H_6 , respectively (methylation effect). C_4H_6 and C_6H_{10} have C_{2h} symmetry, while C_5H_8 has C_s symmetry, and the geometric structures of these hydrocarbons are shown in Fig. 1. Among these three systems, C_4H_6 (1,3-butadiene) is the most investigated molecule under electron collisions.

The presence of shape resonances in the electron interactions with C_4H_6 (1,3-butadiene) was first investigated by Burrow and Jordan [4], through the derivative with respect to energy of the transmitted electron current. The authors assigned the first resonance located at 0.62 eV to the A_u symmetry and the second resonance, located at 2.8 eV, to the B_g symmetry of the C_{2h} group. More recently, Szmytkowski and Kwitniewski measured total cross section for electron collisions with C_4H_6 for impact energies from 0.5 to 370 eV. The authors reported two π^* resonances located at 0.9 and 3.2 eV. Our group carried out calculations for electron collisions with 1,3-butadiene in the static-exchange approximation, for energies from 10 to 60 eV. This work investigated the similarities in the cross sections of some isomers of C_4H_6 , including 1,3-butadiene [5]. In a recent work, Szmytkowski

et al. [6] reported total cross section (TCS) for scattering of electrons by C_5H_8 (2-methyl-1,3-butadiene) for energies from 0.6 to 300 eV. They reported the presence of a π^* shape resonance at 3.4 eV and associated the minimum present in the TCS at around 1.6 eV to a Ramsauer-Townsend minimum. According to the authors, the increase of the TCS at low energy could be partly explained in terms of the permanent dipole moment of the molecule, this behavior being a characteristic of polar molecules. Szmytkowski *et al.* [6] compared the TCSs of C_5H_8 and C_4H_6 and discussed the influence of the methylation effect in the shape and magnitude of the cross sections. They found that the difference in the magnitude of both TCSs was about half of the TCS of C_2H_6 , which corresponds to the cross section of CH_3 . They showed that summing the TCSs of C_4H_6 and CH_3 , the resulting cross section reproduced the TCS of C_5H_8 . They also used this model to estimate the TCS of C_6H_{10} , which has two methyl groups. Regarding the comparison of the positions of the shape resonances, the authors found that the highest π^* shape resonance of C_4H_6 [7], located at around 3.2 eV, is lower for about 0.2 eV with respect to the location of the resonance of C_5H_8 .

In this work we report elastic integral and differential cross sections for the hydrocarbons C_4H_6 , C_5H_8 , and C_6H_{10} . The calculations were done with the Schwinger multichannel method implemented with norm-conserving pseudopotentials. The cross sections were computed in the static-exchange and in the static-exchange plus polarization approximations, for energies up to 15 eV. We focused our attention on the two π^* shape resonances presented in the integral cross section of each one of these molecules and on the minimum reported by the experiment on the TCS of C_5H_8 . We compare our results with the experimental data of C_4H_6 [4,7] and C_5H_8 [6] and with the estimated TCS of C_6H_{10} . We also present a comparison of the differential cross sections at 3, 6, 7, 10, 13, and 15 eV for these hydrocarbons and discuss the oscillatory behavior in terms of the type of the molecular chain.

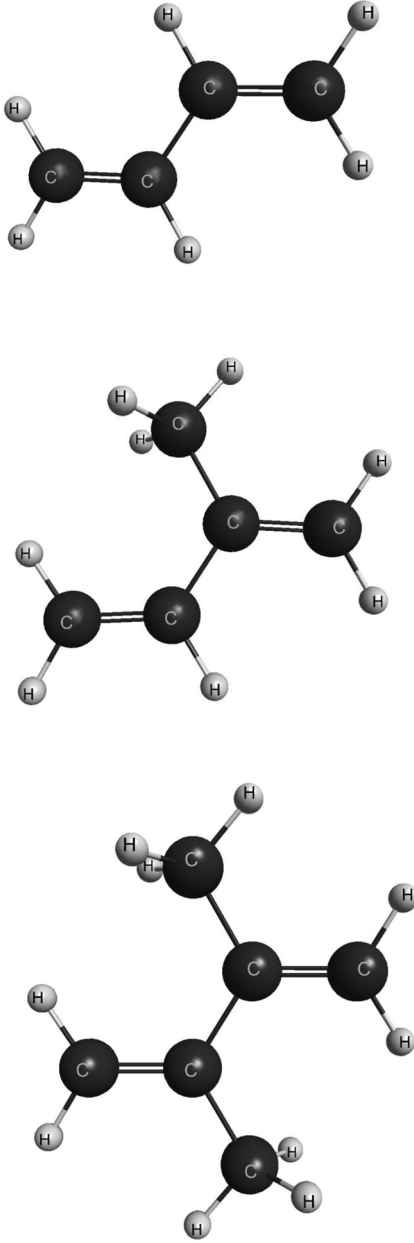


FIG. 1. Geometrical structures of C_4H_6 (top), C_5H_8 (middle), and C_6H_{10} (bottom). Plots made using MACMOLPLT [3].

This paper is organized as follows. Section II presents a short description of the theory and the computational procedures employed in our calculations. In Sec. III we present our results and discussion. Section IV presents a summary of our results and our conclusions.

II. THEORY AND COMPUTATIONAL DETAILS

The elastic cross sections were computed with the Schwinger multichannel method (SMC) [8] and its implementation with pseudopotential (SMCPP) [9] in the parallel version [10]. The SMC and its implementations have been reviewed recently [11], and here we will describe only those aspects of the method that are relevant to the present calculations. The

working expression for the scattering amplitude is given by

$$f(\vec{k}_f, \vec{k}_i) = -\frac{1}{2\pi} \sum_{m,n} \langle S_{\vec{k}_f} | V | \chi_m \rangle (d^{-1})_{mn} \langle \chi_n | V | S_{\vec{k}_i} \rangle, \quad (1)$$

where

$$d_{mn} = \langle \chi_m | A^{(+)} | \chi_n \rangle \quad (2)$$

and

$$A^{(+)} = \frac{1}{2}(PV + VP) - VG_P^{(+)}V + \frac{\hat{H}}{N+1} - \frac{1}{2}(\hat{H}P + P\hat{H}). \quad (3)$$

In the expressions above, $|S_{\vec{k}_i}\rangle$ is an eigenstate of the unperturbed Hamiltonian H_0 , which is the sum of the kinetic energy of the incident electron and the target Hamiltonian. $\{|\chi_m\rangle\}$ represents a set of spin-adapted $(N+1)$ -electron Slater determinants or configuration-state functions (CSFs). V is the interaction potential between the projectile and the target, and $\hat{H} = E - H$, where E is the projectile energy and $H = H_0 + V$ is the scattering Hamiltonian. P is the projection operator onto the open channel of the target, and $G_P^{(+)}$ is the free-particle Green's function projected on the P space.

The present calculations were performed in the static-exchange (SE) and static-exchange plus polarization (SEP) approximations. In the SE approximation, the CSFs are constructed as

$$|\chi_m\rangle = \mathcal{A}_{N+1}[|\Phi_0\rangle \otimes |\varphi_m\rangle], \quad (4)$$

where \mathcal{A}_{N+1} is the antisymmetrization operator of $N+1$ electrons, $|\Phi_0\rangle$ is the target ground state, and $|\varphi_m\rangle$ is a single-particle function (scattering orbital). In the SEP approximation, the configuration space used in the SE approximation is augmented by including CSFs constructed as

$$|\chi_{im}^r\rangle = \mathcal{A}_{N+1}[|\Phi_i^r\rangle \otimes |\varphi_m\rangle], \quad (5)$$

where $|\Phi_i^r\rangle$ account for the single virtual excitations of the target, from the i th occupied (hole) orbital to the r th unoccupied (particle) orbital.

The molecular geometries were optimized at the second order Møller-Plesset perturbation theory (MP2) level of approximation with the aug-cc-pVDZ basis, as implemented in the package GAMESS [12]. The bound state and scattering calculations were done for C_4H_6 and C_6H_{10} in the C_{2h} group and for C_5H_8 in the C_s group. We employed the pseudopotentials of Bachelet *et al.* [13] to represent the core electrons of carbon. To describe the valence electrons of the carbon atom, we used the $5s4p2d$ basis set generated according to Ref. [14]. For the hydrogen atom we used the Dunning [15] $4s/3s$ basis augmented with one p function with exponent equal to 0.75. To represent the particle and scattering orbitals we used modified virtual orbitals (MVOs) [16], which were obtained from the diagonalization of a Fock operator of a cation with charge +6.

In the present implementation of the SMC method, the target is described in the Hartree-Fock approximation. The unbalanced description of the target and the $(N+1)$ -electron system wave functions can result in the overcorrelation, where the consequence is locating the resonances below their

experimental values. In addition, single excitations of the target are double excitations (correlation) for the $(N + 1)$ -electron system. To avoid the overcorrelation, we followed the idea of Winstead and McKoy [17] and chose for each resonance a single scattering orbital represented by a MVO. The choice of MVOs is based on the fact they are compact (valencelike) orbitals, being a good representation for a resonance orbital. Also, with this procedure the polarization effects are described in the same level of the target description (avoiding overcorrelation). In an attempt to balance the inclusion of polarization effects in the resonant symmetries of all hydrocarbons, we computed the cross sections for the A_u and B_g symmetries of the C_{2h} molecules together, as if the molecules were of C_s symmetry. In practice, for the three hydrocarbons, we considered all single excitations that preserved the spatial symmetry of the target, and employed the two lowest MVOs as scattering orbitals. In the construction of the CSFs we included singlet- and triplet-coupled excitations of the target. We obtained 1926 and 4276 CSFs for the $A_u + B_g$ symmetries of C_4H_6 and C_6H_{10} , respectively, and 2983 CSFs for the A'' symmetry of C_5H_8 .

For C_4H_6 , we used 15 191 CSFs for the nonresonant symmetries, namely, A_g and B_u , considering excitations (singlets and triplets) from the 11 hole orbitals to the lowest 71 MVOs. These 71 MVOs were also used as scattering orbitals. For the other C_{2h} molecule, C_6H_{10} , we used 15 275 and 15 274 CSFs for the A_g and B_u symmetries, respectively, considering excitations (singlets and triplets) from the 17 hole orbitals to the lowest 58 MVOs, where these 58 MVOs were also employed as scattering orbitals. In the case of C_5H_8 , we computed the A' symmetry with 15 205 CSFs, obtained by making excitations from the 14 hole orbitals to the lowest 45 MVOs. The 45 MVOs were also used as scattering orbitals.

C_5H_8 has a very small permanent dipole moment with calculated value of 0.27 D. This value agrees very well with the experimental value of 0.25 D [18]. In order to capture the long-range effect of the dipole potential, which is truncated by the Cartesian Gaussian function used as single-particle basis in the SMC method, we used the Born-closure procedure [19]. In short, we considered the scattering amplitude obtained with the SMC method expanded in partial waves up to a l_{\max} , and the amplitude of the dipole potential obtained in the first Born approximation, also expanded in partial waves, from $l_{\max} + 1$ to $+\infty$. Since the long-range potential is more intense at low energies, the value of l_{\max} is energy dependent. We chose this value by looking at the differential cross sections obtained with and without the Born-closure that agree above typically 20°. The values of l_{\max} used in the present calculations are $l_{\max} = 4$ from 1 to 4 eV; $l_{\max} = 5$ from 5 to 9 eV; and $l_{\max} = 6$ from 10 to 15 eV.

III. RESULTS AND DISCUSSION

Figure 2 shows our calculated integral cross sections (ICSs) for C_4H_6 , C_5H_8 , and C_6H_{10} , computed in the SE and SEP approximations. We also show the experimental TCSs for C_4H_6 [7] and for C_5H_8 [6], and the estimated TCS for C_6H_{10} . To estimate the TCS for C_6H_{10} we followed the procedure of Szymtowski *et al.* by using the TCSs data of C_2H_6 [20] and C_5H_8 , and the relation $TCS(C_6H_{10}) =$

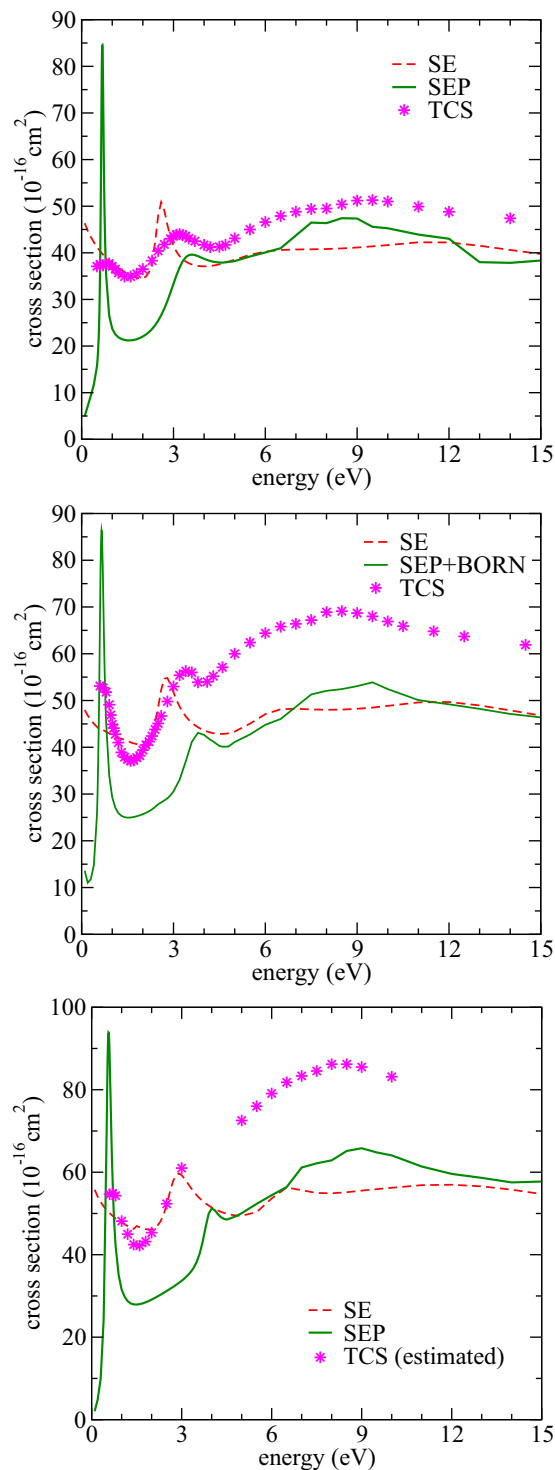


FIG. 2. Integral cross section for scattering of electrons by C_4H_6 (top), C_5H_8 (middle), and C_6H_{10} (bottom), obtained in the SE and SEP approximations. The TCSs of C_4H_6 [7] and C_5H_8 [6] are shown for comparison. The estimated TCS for C_6H_{10} is also shown.

$0.5 \times TCS(C_2H_6) + TCS(C_5H_8)$. In general, our ICSs computed in the SEP approximation follow the shape of the TCSs, but lie below the experiment even at lower energies. The main features present in the computed ICSs in both approximations are the two sharp peaks, which are π^* shape resonances. The resonances for C_4H_6 are located at 2.6 and 6.2 eV, in

TABLE I. Resonances positions obtained in the present SE and SEP calculations and the calculated (VAE_{calc}) and experimental (VAE_{expt}) [4] vertical attachment energies (VAEs). The resonances positions for C₄H₆ [7] and C₅H₈ [6] from the TCSs (Expt.) are also shown. All values are in eV.

	SE		SEP		VAE _{calc}		VAE _{expt}		Expt.	
	π_1^*	π_2^*	π_1^*	π_2^*	π_1^*	π_2^*	π_1^*	π_2^*	π_1^*	π_2^*
C ₄ H ₆	2.6	6.2	0.68	3.6	0.804	3.11	0.62	2.8	0.9	3.2
C ₅ H ₈	2.7	6.5	0.65	3.8	0.841	3.09	–	–	–	3.4
C ₆ H ₁₀	2.9	6.7	0.56	4.0	0.846	3.15	–	–	–	–

the SE approximation and at 0.68 and 3.6 eV, in the SEP approximation. Burrow and Jordan [4] reported these two resonances at 0.62 eV (assigned to the A_u symmetry) and at 2.8 eV (assigned to the B_g symmetry). Szmytkowski and Kwitniewski [7] also reported for this molecule two shape resonances located at 0.9 and 3.2 eV. The SEP calculated values for the resonances positions are in fair agreement with the experimental values. For C₅H₈, the SE calculations locate the resonances at 2.7 and 6.5 eV, while in the SEP approximation the resonances move to 0.65 and 3.8 eV. Recently, Szmytkowski *et al.* reported for this molecule one shape resonance located at 3.4 eV, and a Ramsauer-Townsend minimum located at 1.6 eV. The authors also associated the increase of the TCS at low energy, as a characteristic of the long-range dipole interaction. Although the location of the second resonance in the SEP approximation agrees well with the experiment, our ICS shows no indication of the presence of a Ramsauer-Townsend minimum. We suspect that the rise in the TCS corresponds to the tail of the low-lying resonance, which was not seen by the experiment since the measurements start at 0.6 eV. For the bigger molecule, C₆H₁₀, the resonances in our calculated ICS are located at 2.9 and 6.7 eV, in the SE approximation and at 0.56 and 4 eV, in the SEP approximation. The results are summarized in Table I. The magnitude of the ICSs grows according to the size of the molecule, which is directly related to the methylation effect.

In order to assign the π^* shape resonances to the symmetries of the C_{2h} group, for C₄H₆ and C₆H₁₀, and of the C_s group, for C₅H₈, we carried out the symmetry decomposition of the ICSs shown in Fig. 2. The results are shown in Fig. 3. As we have mentioned above, the cross sections for the resonant symmetries of C₄H₆ and C₆H₁₀ were computed together, considering the molecules as having C_s symmetry. So, the cross section for these two hydrocarbons correspond to $A_u + B_g$ symmetries. For both molecules, the low-lying π_1^* resonance belongs to the A_u symmetry, while the higher-lying π_2^* resonance belong to the B_g symmetry. For C₅H₈ both resonances belong to the A'' symmetry of C_s . It is interesting to note that, although the magnitude of the cross sections differs, their shape are very similar.

According to the SE calculations, the positions of both π_1^* and π_2^* resonances, although very close to each other, follow the size of the molecules: the resonances of C₄H₆ are lower than the resonances of C₅H₈, which in turn are lower than the resonances of C₆H₁₀. We could, in principle, attribute this behavior to the methylation effect. However, this is not true for the resonances obtained in the SEP calculations. The

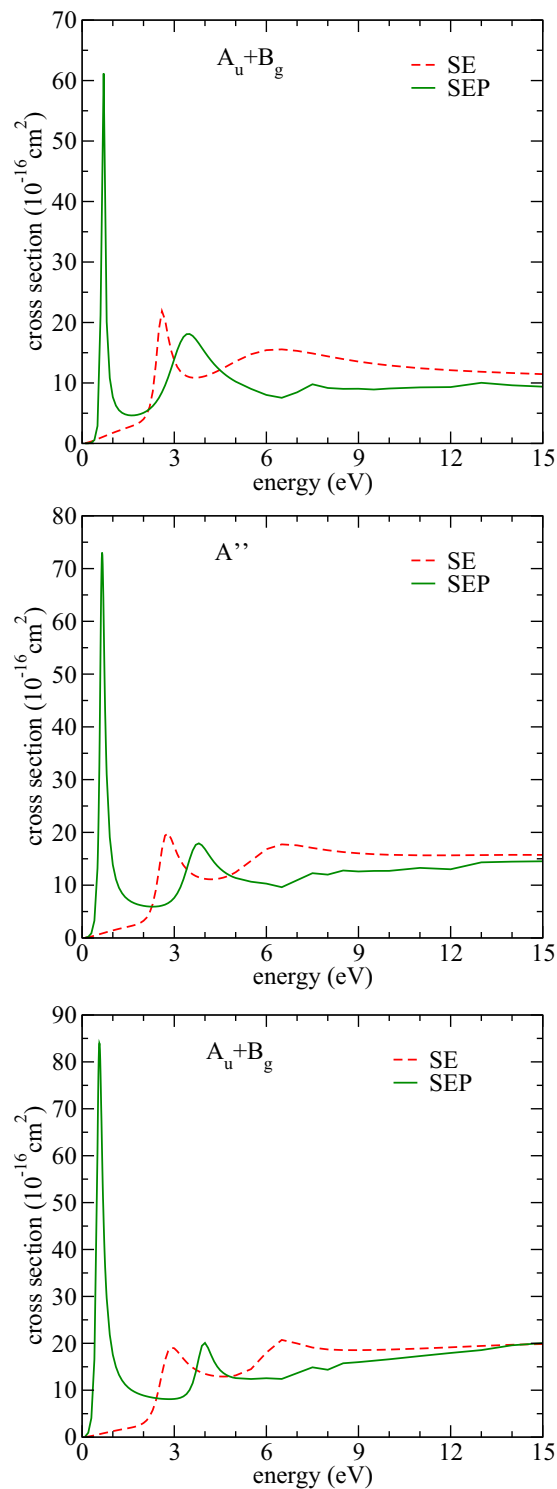


FIG. 3. Symmetry decomposition of the ICS for C₄H₆ (top), C₅H₈ (middle), and C₆H₁₀ (bottom) obtained in the SE and SEP approximations. Only the resonant symmetries are shown.

number of configurations employed in the SEP calculations grows according to the size of the target. It can be observed from Fig. 3 and from Table I that the π_1^* resonances are very close to each other, as well as the π_2^* resonances in both SE and SEP approximations, and the difference in the number of configurations used in the resonant symmetries, although we

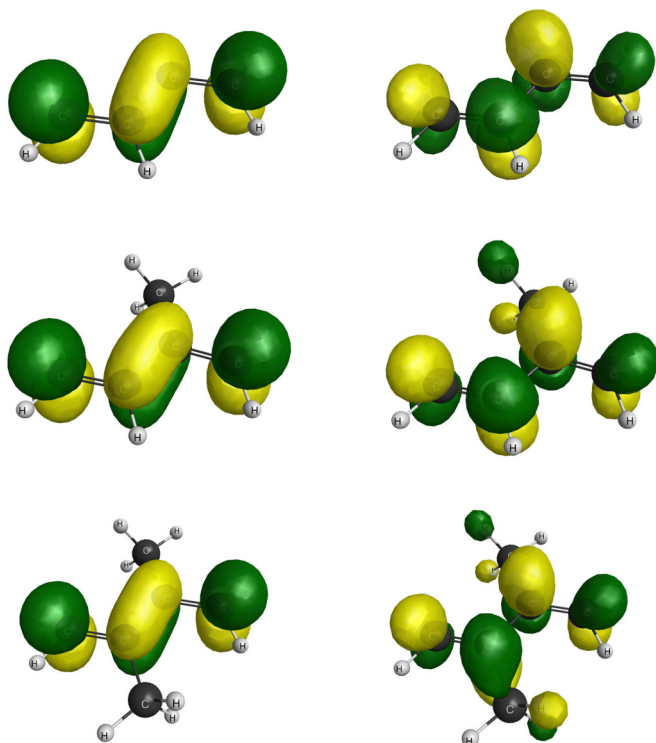


FIG. 4. Molecular orbitals plots for C_4H_6 (top), C_5H_8 (middle), and C_6H_{10} (bottom). For C_4H_6 and C_6H_{10} the orbitals are $\pi_1^*(a_u)$ (left) and $\pi_2^*(b_g)$ (right). For C_5H_8 the orbitals are $\pi_1^*(a'')$ (left) and $\pi_2^*(a'')$ (right). Plots made using MACMOLPLT [3].

tried to balance the calculations, may be responsible for the small differences in the resulting resonance positions, placing them in a different order than in the SE calculation.

We also employed an empirical relation to estimate the resonances positions and to draw the molecular orbitals. We used the program GAMESS to optimize the ground state geometries of the hydrocarbons at the MP2 level of approximation with the 6-31G(d) basis set. The virtual orbital energies (VOEs) were obtained in a Hartree-Fock calculation at the optimized geometries and with the same basis set. The VOEs were used to estimate the vertical attachment energies (VAEs) through the relation [21]

$$\text{VAE} = 0.64795 \times \text{VOE} - 1.4298 \text{ (in eV)}.$$

The results are summarized in Table I, and the molecular orbitals plots are shown in Fig. 4. The positions for the π_1^* resonances obtained in the SEP calculations are lower than the VAEs obtained using the scaling relation, while the values for the SEP positions of the π_2^* resonances are higher than the VAEs. On the other hand, the orbitals shown in the left column of Fig. 4, which correspond to the π_1^* resonances, are very similar to each other. The same occurs with the orbitals corresponding to the π_2^* resonances, shown in the right column of this figure.

The cross sections for the nonresonant symmetries are shown in Figs. 5 and 6. Figure 5 shows the totally symmetric cross sections. The A_g symmetry corresponds to C_4H_6 and C_6H_{10} , and the A' to C_5H_8 . The SE ICSs increase at low energies, while the ICSs with polarization decrease. We have found no indication of a Ramsauer-Townsend minimum in these

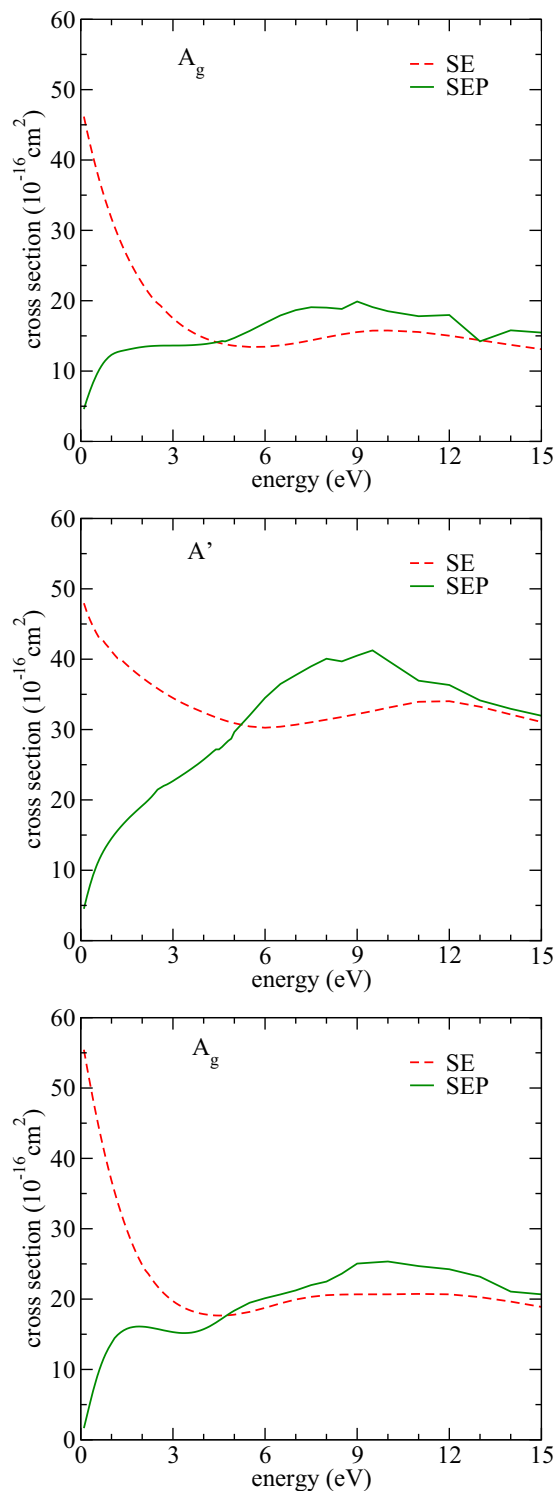


FIG. 5. Cross sections for the A_g symmetry of C_4H_6 (top) and C_6H_{10} (bottom) and for the A' symmetry of C_5H_8 (middle).

cross sections. Another common feature in these SEP ICSs is the presence of a broad structure at around 10 eV. The cross sections for the remaining B_u symmetry of C_{2h} are shown in Fig. 6 for C_4H_6 and C_6H_{10} . Both SEP cross sections present a very broad structure at around 8 eV, which along with the broad structure in the ICSs of A_g , also contribute to the broad structure seen in the ICSs shown in Fig. 2.

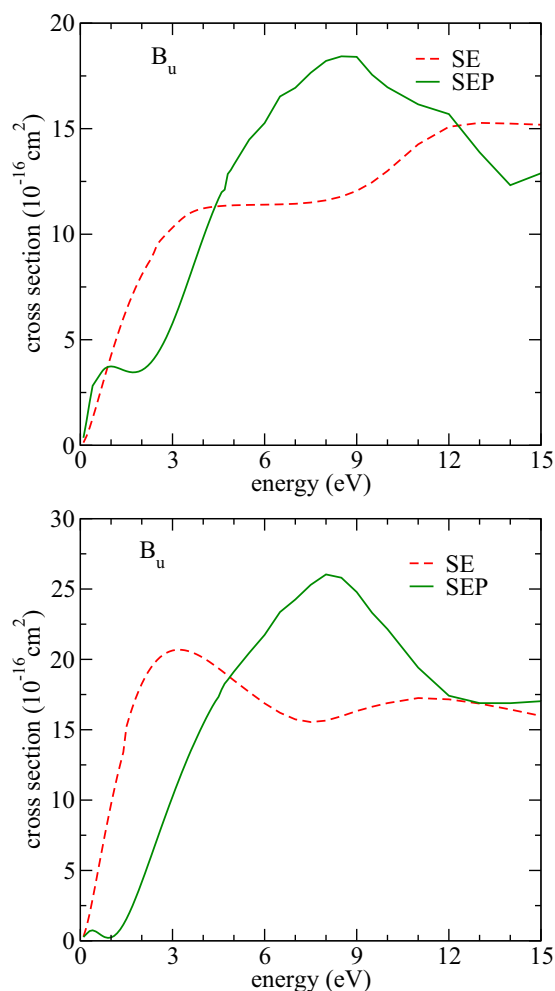


FIG. 6. Cross section for the B_u symmetry of C_4H_6 (top) and C_6H_{10} (bottom).

Figure 7 presents the calculated differential cross sections (DCSs) for the three hydrocarbons at 3, 6, 8, 10, 13, and 15 eV. We show only the DCSs obtained in the SEP approximation. There is a similarity in the oscillatory pattern of the DCSs of C_5H_8 and C_6H_{10} , which present a d -wave pattern. The DCSs for C_4H_6 present a f -wave behavior, which is barely seen at 10 and 13 eV, where the DCSs present a minimum around 90° . The major contribution of a f -wave to the DCS is a characteristic of straight-chain molecules, while the major contribution of d -wave is a characteristic of branched molecules [2].

IV. CONCLUSIONS

We presented integral and differential cross sections for electron scattering by the hydrocarbons 1,3-butadiene (C_4H_6), 2-methyl-1,3-butadiene (C_5H_8), and 2,3-dimethyl-1,3-butadiene (C_6H_{10}). Our calculation were done in the SE and SEP approximations and covered impact energies up to 15 eV. We found two shape resonances for each one of the hydrocarbons. The π_1^* resonances are located very close to each other, the same occurring with the π_2^* resonances. In general, our results for the resonances positions agree well with the experiment. The computed integral cross sections, although smaller than the total cross sections, present the same shape of the experimental data. In addition, the magnitude of the cross sections grows according to their size, as a result of the methylation effect. For C_5H_8 the experiment reported one shape resonance and a Ramsauer-Townsend minimum. The increase observed in the total cross section at low energy was attributed by the authors to a characteristic of the scattering by a polar molecule. Our results shown that this increase is actually a tail of the low-lying shape resonance, and the minimum is in fact a valley between the two resonances. The differential cross sections have different partial wave contributions: for C_4H_6 , which is a straight-chain molecule, the major contribution comes from a f -wave, while for the other two hydrocarbons,

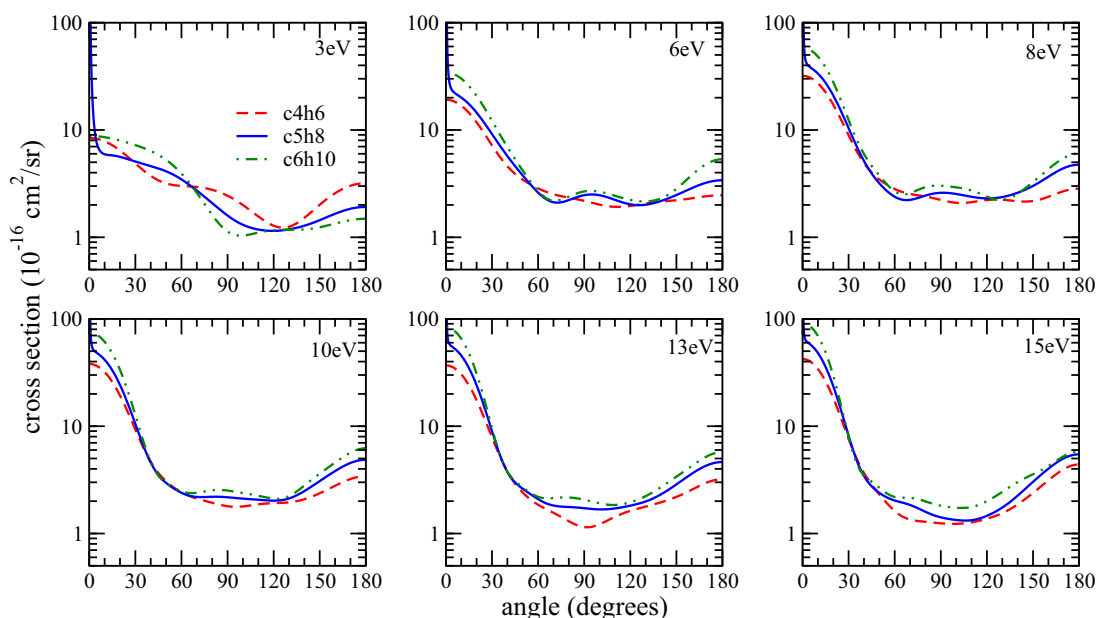


FIG. 7. Differential cross sections for C_4H_6 , C_5H_8 , and C_6H_{10} at 3, 6, 8, 10, 13, and 15 eV. Only the results obtained in the SEP approximation are shown.

which have branched chains, the major contribution comes from a d -wave. This observation is in accord with the results reported by some studies in the literature.

ACKNOWLEDGMENTS

M.B.K and M.H.F.B. acknowledge support from Brazilian agency Conselho Nacional de Desenvolvimento Científico

e Tecnológico (CNPq). D.F.P acknowledges support from Brazilian Agency Coordenação de Aperfeiçoamento de Pessoal de Nível Superior (CAPES). M.H.F.B. also acknowledges support from Financiadora de Projetos (FINEP) (under project CTInfra). The authors acknowledge computational support from Prof. C. M. de Carvalho at LFTC-DFis-UFPR and at LCPAD-UFPR, and from CENAPAD-SP.

-
- [1] For a summary of electron collisions with hydrocarbons see, for example, L. Chiari, A. Zecca, F. Blanco, G. García, and M. J. Brunger, *J. Chem. Phys.* **144**, 084301 (2016).
- [2] M. H. F. Bettega, C. Winstead, and V. McKoy, *Phys. Rev. A* **82**, 062709 (2010); M. H. F. Bettega, C. Winstead, V. McKoy, A. Jo, A. Gauß, J. Tanner, L. R. Hargreaves, and M. A. Khakoo, *ibid.* **84**, 042702 (2011); K. Fedus, C. Navarro, L. R. Hargreaves, M. A. Khakoo, F. M. Silva, M. H. F. Bettega, C. Winstead, and V. McKoy, *ibid.* **90**, 032708 (2014).
- [3] B. M. Bode and M. S. Gordon, *J. Mol. Graph. Mod.* **16**, 133 (1998).
- [4] P. D. Burrow and K. D. Jordan, *Chem. Phys. Lett.* **36**, 594 (1975).
- [5] A. R. Lopes, M. A. P. Lima, L. G. Ferreira, and M. H. F. Bettega, *Phys. Rev. A* **69**, 014702 (2004).
- [6] Cz. Szmytkowski, S. Stefanowska, M. Zawadzki, E. Ptasíńska-Denga, and P. Mozejko, *Phys. Rev. A* **94**, 042706 (2016).
- [7] Cz. Szmytkowski and S. Kwitnewski, *J. Phys. B* **36**, 2129 (2003).
- [8] K. Takatsuka and V. McKoy, *Phys. Rev. A* **24**, 2473 (1981); **30**, 1734 (1984).
- [9] M. H. F. Bettega, L. G. Ferreira, and M. A. P. Lima, *Phys. Rev. A* **47**, 1111 (1993).
- [10] J. S. dos Santos, R. F. da Costa, and M. T. do N. Varella, *J. Chem. Phys.* **136**, 084307 (2012).
- [11] R. F. da Costa, M. T. do N. Varella, M. H. F. Bettega, and M. A. P. Lima, *Eur. Phys. J. D* **69**, 159 (2015).
- [12] M. W. Schmidt, K. K. Baldridge, J. A. Boatz, S. T. Elbert, M. S. Gordon, J. H. Jensen, S. Koseki, N. Matsunaga, K. A. Nguyen, S. J. Su, T. L. Windus, M. Dupuis, and J. A. Montgomery, *J. Comput. Chem.* **14**, 1347 (1993).
- [13] G. B. Bachelet, D. R. Hamann, and M. Schlüter, *Phys. Rev. B* **26**, 4199 (1982).
- [14] M. H. F. Bettega, A. P. P. Natalense, M. A. P. Lima, and L. G. Ferreira, *Int. J. Quan. Chem.* **60**, 821 (1996).
- [15] T. H. Dunning Jr., *J. Chem. Phys.* **53**, 2823 (1970).
- [16] C. W. Bauschlicher Jr., *J. Chem. Phys.* **72**, 880 (1980).
- [17] C. Winstead and V. McKoy, *Phys. Rev. A* **57**, 3589 (1998).
- [18] See <http://cccbdb.nist.gov> for the experimental value of the dipole moment for C_5H_8 .
- [19] E. M. de Oliveira, R. F. da Costa, S. d'A. Sanchez, A. P. P. Natalense, M. H. F. Bettega, M. A. P. Lima, and M. T. do N. Varella, *Phys. Chem. Chem. Phys.* **15**, 1682 (2013).
- [20] Cz. Szmytkowski and S. Kwitnewski, *J. Phys. B* **28**, 4291 (1995).
- [21] S. S. Staley and J. T. Strnad, *J. Phys. Chem.* **98**, 161 (1994).